Acta Cryst. (1984). B40, 228–237

The Modulated Structure of Intermediate Plagioclase Feldspar $Ca_xNa_{1-x}Al_{1+x}Si_{3-x}O_8$

BY AKIJI YAMAMOTO AND HIROMOTO NAKAZAWA

National Institute for Research in Inorganic Materials, Namiki, Sakura-Mura, Niihari-Gun, Ibaraki, 305 *Japan*

AND MASAO KITAMURA AND NOBUO MORIMOTO

Department of Geology and Mineralogy, Kyoto University, Sakyo-Ku, Kyoto, 606 *Japan*

(*Received* 5 *July* 1983; *accepted* 15 *December* 1983)

Abstract

The modulated structure of labradorite (An_{52}) has been refined within the harmonic approximation using the intensity data collected by Klein [Horst, Tagai, Korekawa & Jagodzinski (1981). *Z. Kristallogr.* **157**, 233–250]. The analysis is based on the four-dimensional triclinic space group with centering translations which is group-theoretically equivalent to $P^{P\bar{1}}_{1}$. The restricted least-squares method with two kinds of penalty functions has been employed to keep the occupation probability and the bond lengths within crystal-chemically reasonable ranges. This method gave smooth convergence of the R factors from 0·207 to 0·065 for 1633 observed main (a) and from 0·83 to 0·094 for 3102 observed e_1-satellite reflections after 18 cycles. The average bond distances between the tetrahedral Al/Si and four neighboring O atoms show distinct periodic substitutions of Al and Si, while the substitutional modulation of the Ca/Na site is weak. These results are consistent with the model proposed by Kitamura & Morimoto [*Phys. Chem. Miner.* (1977), **1**, 199–212]. With the anharmonic terms taken into account, a reasonable interpretation of the diffraction aspect of the higher-order satellite reflections has been made by the present structure determination and the phase fluctuation of the modulation waves, which is important in evaluation of the higher-order satellite intensity. The present results indicate that the most probable structure of labradorite is a modulated structure with albite-like (An_{20}) and anorthite-like (An_{80}) regions. The anorthite-like regions in an antiphase relation are coherently separated by the albite-like regions.

Introduction

Plagioclase feldspars, $Ca_xNa_{1-x}Al_{1+x}Si_{3-x}O_8$, which constitute a solid solution between anorthite (An), $CaAl_2Si_2O_8$, and albite (Ab), $NaAlSi_3O_8$, show modulated structures in the range of about An_{25}–An_{75}. The modulated structures have been analyzed by X-ray diffraction, resulting in several different models. Toman & Frueh (1976) studied labradorite (An_{55}) based on displacive modulation for all atoms and substitutional modulation for Ca/Na sites and obtained the Al/Si distribution from the periodic change in the bond distances. Their result shows that the Al-rich regions alternate with Si-rich regions twice in a modulated-structure period. On the other hand, the Ca/Na distribution is homogeneous in both regions. Horst, Tagai, Korekawa & Jagodzinski (1981) also studied labradorite (An_{52}), based on an antiphase relation of two similar structure units with notably disordered Al/Si and Ca/Na distributions. In both models, there are no albite-like and anorthite-like regions as a whole because of the homogeneous Ca/Na distribution and/or the disordered Al/Si distribution. From the crystal-chemical viewpoint, it is natural to consider that Na is rich in the Si-rich regions forming the albite-like regions, and Ca is rich in the Al-rich regions forming the anorthite-like regions. In fact, Kitamura & Morimoto (1975, 1977) presented a modulated structure consisting of albite-like and anorthite-like regions for bytownite (An_{73}) by an X-ray diffraction study. This structure was confirmed by the lattice imaging of labradorite (An_{54}) by high-resolution electron microscopy (Morimoto, Nakajima & Kitamura, 1975; Nakajima, Morimoto & Kitamura, 1977). The change of the modulated structures with composition was also discussed for the intermediate plagioclase based on the antiphase-domain relation of the model presented by Kitamura & Morimoto (Morimoto *et al.*, 1975; Morimoto, 1979).

Large R factors for the satellite reflections in all the previous analyses, however, indicate that the superstructure of the intermediate plagioclase has not been completely solved. In this paper, we have applied the analytical method of modulated structures based on the four-dimensional description (de Wolff, 1974; Janner & Janssen, 1977; Yamamoto, 1982*a*) to the analysis of An_{52}. In order to analyze this complex structure, we have introduced a new restricted least-squares technique which uses the penalty function to keep the interatomic distances within a crystal-chemically reasonable range. The analysis has been carried out by using the X-ray data collected by Klein (Horst, Tagai, Korekawa & Jagodzinski, 1981; Tagai, 1980), which include 1640 main and 3220 satellite reflections.

0108-7681/84/030228-10$01.50

Modulation wave

The plagioclase feldspar has a triclinic average structure. Therefore, the intermediate plagioclase has the triclinic space group $P\bar{1}$ or $P1$. We assume the centrosymmetric $P\bar{1}$. In this case the possible four-dimensional space group is only $P^{P\bar{1}}_{\bar{1}}$ (de Wolff, Janssen & Janner, 1981). To facilitate comparison with the previous results, however, the conventional anorthite cell has been used in this study. The cell dimensions of labradorite are then $a = 8{\cdot}178\,(1)$, $b = 12{\cdot}865\,(1)$, $c = 14{\cdot}218\,(1)$ Å, $\alpha = 93{\cdot}53\,(1)$, $\beta = 116{\cdot}21\,(1)$, $\gamma = 89{\cdot}92\,(1)^\circ$ (Horst *et al.*, 1981). All reflections with diffraction vector $\mathbf{h}$ are designated with four integers h_1, h_2, h_3, h_4 by using $\mathbf{h} = h_1\mathbf{a}^* + h_2\mathbf{b}^* + h_3\mathbf{c}^* + h_4\mathbf{k}$, where $\mathbf{a}^*$, $\mathbf{b}^*$, $\mathbf{c}^*$ are the unit vectors reciprocal to $\mathbf{a}, \mathbf{b}, \mathbf{c}$ and $\mathbf{k} = k_1\mathbf{a}^* + k_2\mathbf{b}^* + k_3\mathbf{c}^*$ is the (basic) wavevector of the modulation waves. The components k_1, k_2, k_3 depend on the chemical composition of labradorite (Bown & Gay, 1958). In the present case (An_{52}), $k_1 = 0{\cdot}061$, $k_2 = 0{\cdot}044$ and $k_3 = -0{\cdot}222$ (Horst *et al.*, 1981). Since the unit cell employed is not primitive, we find systematic-extinction rules $h_1 + h_2 + h_3 = 2n$, $h_1 + h_2 + h_4 = 2n$, $h_3 + h_4 = 2n$ for general reflections.

The corresponding unit vectors in the four-dimensional lattice are given by $\mathbf{a}_1 = \mathbf{a} - k_1\mathbf{d}$, $\mathbf{a}_2 = \mathbf{b} - k_2\mathbf{d}$, $\mathbf{a}_3 = \mathbf{c} - k_3\mathbf{d}$ and $\mathbf{a}_4 = \mathbf{d}$ where $\mathbf{d}$ is the unit vector perpendicular to the usual three-dimensional space (spanned by $\mathbf{a}, \mathbf{b}, \mathbf{c}$) while their reciprocal vectors are $\mathbf{b}_1 = \mathbf{a}^*$, $\mathbf{b}_2 = \mathbf{b}^*$, $\mathbf{b}_3 = \mathbf{c}^*$ and $\mathbf{b}_4 = \mathbf{k} + \mathbf{d}$ (de Wolff, 1974). In the four-dimensional description of the modulated structures, the diffraction vector $\mathbf{h}$ is regarded as the projection of the four-dimensional vector $\mathbf{h}' = \sum_{i=1}^{4} h_i\mathbf{b}_i$ onto the usual three-dimensional space. The observed extinction rules mentioned above are explained by the existence of the centering translations $(\mathsf{E}|\frac{1}{2}, \frac{1}{2}, \frac{1}{2}, 0)$, $(\mathsf{E}|\frac{1}{2}, \frac{1}{2}, 0, \frac{1}{2})$, $(\mathsf{E}|0, 0, \frac{1}{2}, \frac{1}{2})$ (Yamamoto, 1982*a*, *b*, and see also Appendix 2), where the translation vector in four-dimensional space is represented by its $\mathbf{a}_1, \mathbf{a}_2, \mathbf{a}_3, \mathbf{a}_4$ components. Since the space group of the average structure is triclinic, the four-dimensional space group of the modulated structure with these centering translations must be equivalent to the space group $P^{P\bar{1}}_{\bar{1}}$ with a primitive lattice.† In fact this is equivalent to $P^{P\bar{1}}_{\bar{1}}$ as shown in Appendix 1.

In the fundamental structure, there are 13 independent atoms: one Ca/Na, four tetrahedral Al/Si and eight O atoms. However, because the split-atom model has been employed for the Ca/Na sites in this study (Fleet, Chandrasekhar & Megaw, 1966), altogether 14 independent sites are present. All the sites are of the general position, so that the modulation waves do not suffer any limitation in their forms except that the total occupation probability of the split sites must be unity. The displacive modulation for all atoms and the substitutional modulation for each Ca/Na site have been considered, though the substitutional modulation for the Al/Si site has been neglected because of the small difference between the atomic scattering factors for Al and Si atoms.

The displacement from the fundamental structure and the occupation probability of the μth independent atom ($\mu = 1, \ldots, 14$) are represented by the Fourier series:

$$u_i^\mu(\bar{x}_4^\mu) = \tfrac{1}{2}\sum_n [u_{in}^\mu \exp(2\pi i n\bar{x}_4^\mu) + \text{c.c.}] \quad (1)$$

$$P^\mu(\bar{x}_4^\mu) = \tfrac{1}{2}\sum_n [P_n^\mu \exp(2\pi i n\bar{x}_4^\mu) + \text{c.c.}]. \quad (2)$$

The notation is the same as that in Yamamoto (1982*a*). The isotropic temperature factor is given by

$$B^\mu(\bar{x}_4^\mu) = \tfrac{1}{2}\sum_n [B_n^\mu \exp(2\pi i n\bar{x}_4^\mu) + \text{c.c.}], \quad (3)$$

while the anisotropic temperature factor is represented by

$$B_{ij}^\mu(\bar{x}_4^\mu) = \tfrac{1}{2}\sum_n [B_{ijn}^\mu \exp(2\pi i n\bar{x}_4^\mu) + \text{c.c.}]. \quad (4)$$

The complex amplitudes up to $n = 1$ are taken as independent parameters in (1)–(4) because available reflections are only main (a) and first-order (e_1) satellite reflections. The modulation waves for the remaining atoms are obtained from (1)–(4) by the inversion $(\bar{1}|0, 0, 0, 0)$ and the centering translations mentioned above. In particular, the centering translation $(\mathsf{E}|\tau_1, \tau_2, \tau_3, \tau_4)$ transforms the modulation function $u_i^\mu(\bar{x}_4^\mu)$ into

$$u_i^\lambda(\bar{x}_4^\lambda) = \tfrac{1}{2}\sum_n \{u_{in}^\mu \exp[2\pi i n(\bar{x}_4^\lambda - \tau_4)] + \text{c.c.}\}$$
$$= u_{in}^\mu(\bar{x}_4^\lambda - \tau_4),$$

where λ is the index of the atom transformed from the atom μ by the centering translation (Yamamoto, 1982*a*). This means that the modulation function of the λth atom is obtained from the modulation function of the μth atom with a shift of τ_4 along the $\mathbf{a}_4$ axis or, in other words, the nth-order harmonic of $u_i^\lambda(\bar{x}_4^\lambda)$ has the phase shift $2\pi n\tau_4$. This agrees with the conditions found by Korekawa & Jagodzinski (1967) which are necessary to explain the extinction rules. The centering translations, therefore, show that the modulation waves of the sites obtained from independent sites by translations $(\mathbf{a} + \mathbf{b})/2$ and $\mathbf{c}/2$ are given from those of the independent site by a shift of $\frac{1}{2}$ along the $\mathbf{a}_4$ axis while the modulation waves of the site obtained by $(\mathbf{a} + \mathbf{b} + \mathbf{c})/2$ are the same as those of the independent site.

Refinement method

In order to constrain the occupation probability and bond lengths within reasonable ranges, the penalty-function method has been employed in which the sum of the squared weighted R factor, $(R_w)^2 = \sum w(F_o - F_c)^2 / \sum wF_o^2$, and squared penalty functions

† No space-group symbol has been proposed for the nonstandard setting with such centering translations.

mentioned later is minimized by the least-squares method.

In the substitutional modulation, the occupation probability of each atomic site, $P^{\mu}(\bar{x}_4^{\mu})$, must be constrained within a physically reasonable range: $0 \leq P^{\mu}(\bar{x}_4^{\mu}) \leq 1$. In order to keep the occupation probability of each Ca/Na site within this range, a penalty function (PF_1) has been used (Yamamoto & Inoue, 1981). An additional penalty function (PF_2) has been introduced to restrain the bond length between an Si/Al atom and its neighboring O atom or the average bond length between an Si/Al atom and its four neighboring O atoms within a crystal-chemically reasonable range.

The first penalty function is defined by

$$(PF_1)^2 = \frac{g_1}{N} \sum_{\mu} \int_0^1 dt \{r^{\mu}\}^2, \tag{5}$$

where $t = \bar{x}_4^{\mu} - \mathbf{k}.\bar{\mathbf{x}}^{\mu}$ ($\bar{\mathbf{x}}^{\mu}$ being the position vector of the μth atom in the fundamental structure), r^{μ} takes a value $P^{\mu}(\bar{x}_4^{\mu})$ for $P^{\mu}(\bar{x}_4^{\mu}) < 0$, $1 - P^{\mu}(\bar{x}_4^{\mu})$ for $1 < P(\bar{x}_4^{\mu})$ and zero otherwise, μ runs over all the independent atoms in the unit cell, the number of which is N and g_1 is the weight for the penalty function, for which an appropriate value is given in the refinement.

The second penalty function is given by

$$(PF_2)^2 = \frac{g_2}{M} \sum_{\nu=1}^{M} \int_0^1 dt \left\{\frac{S^{\nu}}{\Delta d^{\nu}}\right\}^2, \tag{6}$$

where $\Delta d^{\nu} = d^{\nu}_{max} - d^{\nu}_{min}$, S^{ν} is $d^{\nu}_{min} - d^{\nu}(t)$ for $d^{\nu}(t) < d^{\nu}_{min}$ and $d^{\nu}(t) - d^{\nu}_{max}$ for $d^{\nu}_{max} < d^{\nu}(t)$, d^{ν}_{min} and d^{ν}_{max} being lower and upper limits of the νth average interatomic distance, $d^{\nu}(t)$, which is a function of t, and zero otherwise. M is the number of average interatomic distances to be constrained and g_2 is the weight for the penalty function. The average bond distance of N_p bonds in the usual three-dimensional space is calculated from

$$d^{\nu}(t) = \frac{1}{N_p} \sum_{(\mu\lambda)} \left[\sum_{ij=1}^{3} (x_i^{\lambda} - x_j^{\mu}) g_{ij} (x_j^{\lambda} - x_j^{\mu})\right]^{1/2}, \tag{7}$$

where x_i^{λ} and $x_i^{\mu} (i = 1, 2, 3)$ are the atomic coordinates of a specified pair at $\bar{x}_4^{\lambda} = \mathbf{k}.\bar{\mathbf{x}}^{\lambda} + t$ and $\bar{x}_4^{\mu} = \mathbf{k}.\bar{\mathbf{x}}^{\mu} + t$ and g_{ij} are metric tensors in the usual three-dimensional space. $\sum_{(\mu\lambda)}$ represents the summation over specified pairs, the number of which is N_p. Since only the coordinates of the independent atoms are determined in the refinement, in the calculation of (7), we need to calculate coordinates of some (λth) atom related to a (μth) independent atom by a symmetry operator $(R|\tau_1, \tau_2, \tau_3, \tau_4)$ in four-dimensional space group. These are obtained from $x_i^{\lambda}(\bar{x}_4^{\lambda}) = \sum_{j=1}^{4} R_{ij} x_j^{\mu}(x_4') + \tau_i$ where $x_4' = (R^{-1})_{44}\bar{x}_4^{\lambda} - \tau_4$. Using these penalty functions and taking appropriate values for g_1 and g_2, we minimize $\chi^2 = (R_w)^2 + (PF_1)^2 + (PF_2)^2$ by the least-squares method.

As mentioned in *Modulation wave*, we consider the substitutional modulation for the split Ca/Na sites. Then the total occupation probability of these sites must be unity:

$$P^{Na(1)}(\bar{x}_4^1) + P^{Ca(1)}(\bar{x}_4^1) + P^{Na(2)}(\bar{x}_4^2) + P^{Ca(2)}(\bar{x}_4^2) = 1,$$

where $\bar{x}_4^1 = \mathbf{k}.\bar{\mathbf{x}}^1 + t$, $\bar{x}_4^2 = \mathbf{k}.\bar{\mathbf{x}}^2 + t$, $\bar{\mathbf{x}}^1$ and $\bar{\mathbf{x}}^2$ are the position vectors of the split sites in the fundamental structure (see *Structure refinement*). This leads to

$$P_0^{Ca(1)} + P_0^{Na(1)} + P_0^{Ca(2)} + P_0^{Na(2)} = 1 \tag{8}$$

$$P_n^{Ca(1)} + P_n^{Na(1)} + P_n^{Ca(2)} + P_n^{Na(2)} = 0 \quad (n \geq 1), \tag{9}$$

where $P_n^{Ca(i)}$ and $P_n^{Na(i)}$ ($i = 1, 2$; $n \geq 0$) are the nth-order Fourier amplitudes of the occupation probabilities of Ca and Na atoms in the split sites. The refinement of the Fourier amplitudes under the constraint conditions (8) and (9) can be made by introducing the following independent parameters, $z_n^1 - z_n^4$.

$$\begin{pmatrix} P_n^{Ca(1)} \\ P_n^{Na(1)} \\ P_n^{Ca(2)} \\ P_n^{Na(2)} \end{pmatrix} = \begin{pmatrix} 1 & 1 & 1 & 1 \\ 1 & -1 & 1 & -1 \\ 1 & 1 & -1 & -1 \\ 1 & -1 & -1 & 1 \end{pmatrix} \begin{pmatrix} z_n^1 \\ z_n^2 \\ z_n^3 \\ z_n^4 \end{pmatrix}. \tag{10}$$

Conditions (8) and (9) are fulfilled by fixing z_0^1 and z_1^1 at $\frac{1}{4}$ and 0.

In addition, from the chemical composition of An_{52}, we have $P_0^{Ca(1)} + P_0^{Ca(2)} = 0{\cdot}52$, which is realized by $z_0^2 = 0{\cdot}01$. For Al/Si and O sites, we have $P_0 = 1$, $P_n = 0$ ($n \geq 1$) and we use the atomic scattering factor of Si for Al/Si sites. Remaining parameters are refined together with the positional and thermal parameters. Except for the symmetry and the constraint conditions mentioned above, the method of analysis is similar to the previous ones (Yamamoto & Nakazawa, 1982; Yamamoto, 1982*b*). It is, however, worth mentioning that, as shown in Appendix 2, the structure factor can be calculated without taking into account the centering translations because the extinct reflections due to these translations are usually not used in the analysis while these translations are necessary to calculate some bond distances as stated above.

Structure refinement

The positional parameters of the fundamental structure were taken from those of the average structure of An_{55} (Toman & Frueh, 1973). Because the split Ca/Na sites were assumed in the structure, their positional parameters were taken from bytownite (model 3 in Fleet, Chandrasekhar & Megaw, 1966).

Table 1. *The atomic positions in the fundamental structure used in the analysis.*

The parameters are taken from Toman & Frueh (1973) except for those of Ca/Na. The parameters of the split Ca/Na sites are taken from Fleet *et al.* (1966).

Site		$\bar{x}_1$	$\bar{x}_2$	$\bar{x}_3$
Ca/Na(1)		0·2665	−0·0162	0·0860
Ca/Na(2)		0·2707	0·0380	0·0414
Al/Si(1)	T_{1o}	0·0059	0·1649	0·1077
Al/Si(2)	T_{1m}	0·0043	0·8191	0·1164
Al/Si(3)	T_{2o}	0·6859	0·1096	0·1593
Al/Si(4)	T_{2m}	0·6814	0·8802	0·1782
O(1)	O_{A1}	0·0072	0·1280	0·4892
O(2)	O_{A2}	0·5835	0·9959	0·1378
O(3)	OB_o	0·8130	0·1052	0·0929
O(4)	OB_m	0·8194	0·8554	0·1226
O(5)	OC_o	0·0163	0·2948	0·1398
O(6)	OC_m	0·0135	0·6902	0·1080
O(7)	OD_o	0·1960	0·1073	0·1920
O(8)	OD_m	0·1928	0·8670	0·2160

The positional parameters of the fundamental structure are given in Table 1. The harmonic approximation was made because the higher-order satellite reflections were not included in the data used. The refinement was initiated from $u^{\mu}_{i0}=0$, $u^{\mu}_{i1}=0{\cdot}005+i0{\cdot}005$ $(i=1,2,3)$, $B^{\mu}_0=1$, $B^{\mu}_1=0$ Å^2 $(\mu=1,2,\ldots,14)$, $z^3_0=z^4_0=0$ and $z^i_1=0$ $(i=2,3,4)$ by use of the isotropic temperature factor. The initial R factors were 0·39 for all observed reflections, 0·207 for 1633 observed main (a) and 0·83 for 3102 observed satellite (e_1) reflections and the penalty functions were $PF_1=0$, $PF_2=0{\cdot}34$ with $g_1=g_2=4$, $d_{min}=1{\cdot}60$, $d_{max}=1{\cdot}76$ Å for all the Al/Si–O bonds. The second penalty function, PF_2, was used to keep individual Al/Si–O distances within this range. [In this case, $N_p=1$ in (7).]

The first refinement was made by fixing B^{μ}_1 and gave $R=0{\cdot}116$, $R_0=0{\cdot}091$, $R_1=0{\cdot}175$, $PF_1=PF_2=0$ after nine cycles (R_0 and R_1 represent the R factors for the main and e_1-satellite reflections hereafter). In the following steps, the average Al/Si–O distances were restrained between d_{min} and d_{max} mentioned above. In the next two cycles, all parameters, including B^{μ}_1, were refined and $R=0{\cdot}111$, $R_0=0{\cdot}090$, $R_1=0{\cdot}161$, $PF_1=PF_2=0$ were obtained.

The final refinement was made by using the anisotropic temperature factor. After seven cycles, the refinement converged at $R=0{\cdot}074$, $R_0=0{\cdot}065$, $R_1=0{\cdot}094$, $PF_1=PF_2=0$. The R factors including nonobserved 7 main and 118 satellite reflections were $R=0{\cdot}078$, $R_0=0{\cdot}066$, $R_1=0{\cdot}105$. The latter values can be compared with the previous R factors obtained by Horst *et al.* (1981) using the same intensity data: $R=0{\cdot}080$, $R_0=0{\cdot}066$ and $R_1=0{\cdot}182$. The present model includes many parameters compared with the model by Horst *et al.*, but the significance test on these models (Hamilton, 1965) confirms that the present model is significant with a confidence larger than 99·5%. The final parameters are shown in Tables 2 and 3.*

Throughout the refinement, unit weight was used for observed reflections and zero weight for nonobserved reflections.

Table 2. *The Fourier amplitudes of the displacement* ($\times10^4$) *in* An_{52}

Re u_{in} and Im u_{in} represent the real and imaginary parts of the complex amplitude u_{in}.

		Re u_{i0}	Re u_{i1}	Im u_{i1}
Ca/Na(1)	u_1	13 (9)	−31 (9)	−21 (14)
	u_2	18 (24)	126 (23)	250 (35)
	u_3	−59 (22)	−85 (19)	−103 (32)
Ca/Na(2)	u_1	2 (8)	−40 (9)	8 (12)
	u_2	−97 (7)	−4 (9)	48 (7)
	u_3	83 (6)	−21 (6)	8 (6)
Al/Si(1)	u_1	6 (1)	−25 (2)	−46 (1)
	u_2	−2 (1)	23 (1)	80 (1)
	u_3	−8 (1)	31 (1)	13 (1)
Al/Si(2)	u_1	−12 (1)	24 (2)	58 (1)
	u_2	−16 (1)	5 (1)	73 (1)
	u_3	−4 (1)	−28 (1)	−3 (1)
Al/Si(3)	u_1	5 (1)	−48 (2)	−17 (1)
	u_2	−1 (1)	−26 (1)	−47 (1)
	u_3	−8 (1)	7 (1)	13 (1)
Al/Si(4)	u_1	8 (1)	19 (2)	37 (1)
	u_2	−5 (1)	−20 (1)	−58 (1)
	u_3	1 (1)	−25 (1)	0 (1)
O(1)	u_1	−42 (4)	73 (6)	22 (6)
	u_2	19 (2)	−10 (3)	−122 (3)
	u_3	5 (1)	9 (3)	−18 (2)
O(2)	u_1	−8 (3)	−30 (5)	32 (4)
	u_2	−28 (1)	13 (3)	−68 (2)
	u_3	14 (2)	1 (3)	−3 (2)
O(3)	u_1	−3 (3)	−78 (6)	−28 (5)
	u_2	10 (2)	−12 (3)	50 (2)
	u_3	21 (2)	31 (3)	3 (3)
O(4)	u_1	−19 (4)	11 (7)	87 (5)
	u_2	−16 (2)	11 (3)	−5 (3)
	u_3	4 (2)	−92 (4)	39 (3)
O(5)	u_1	−21 (3)	26 (6)	−87 (5)
	u_2	−23 (2)	70 (3)	79 (2)
	u_3	−8 (2)	46 (3)	16 (2)
O(6)	u_1	21 (4)	2 (6)	111 (5)
	u_2	−13 (2)	44 (3)	96 (2)
	u_3	7 (2)	−27 (3)	−37 (2)
O(7)	u_1	32 (3)	83 (6)	−32 (5)
	u_2	6 (2)	−9 (3)	80 (2)
	u_3	0 (2)	18 (3)	5 (2)
O(8)	u_1	−31 (4)	−77 (6)	16 (5)
	u_2	0 (2)	−18 (3)	72 (2)
	u_3	−5 (2)	−25 (3)	−9 (2)

Table 3. *The occupational parameters for the* Ca/Na *sites* ($\times10^2$)

z^3_0	z^4_0	z^2_1	z^3_1	z^4_1
2 (4)	4 (14)	5 (1) + *i*3 (1)	−1 (5) − *i*3 (5)	−4 (18) − *i*8 (16)

Modulated structure

The substitutional modulation of the Al/Si sites is not studied directly by evaluating the occupation

* Lists of structure factors and thermal parameters have been deposited with the British Library Lending Division as Supplementary Publication No. SUP 39127 (23 pp.). Copies may be obtained through The Executive Secretary, International Union of Crystallography, 5 Abbey Square, Chester CH1 2HU, England.

probability of Si or Al atoms but by using the interatomic distances between the Al/Si atoms and their four neighboring O atoms. As is well known (Ribbe & Gibbs, 1969), the average interatomic distances between the Al/Si atom and its four neighboring O atoms vary linearly from 1·605 Å for pure Si to 1·757 Å for pure Al in feldspars. The function $d^{\nu}(t)$ in (7) represents the change of the interatomic distance in the modulated structure: the interatomic distance of the μth atom located at $\bar{\mathbf{x}}=\bar{\mathbf{x}}^{\mu}+\bar{\mathbf{x}}_1$ ($\bar{\mathbf{x}}_1$ being a lattice vector) in the fundamental structure and its neighboring atoms is given by $d^{\nu}(\mathbf{k}.\bar{\mathbf{x}}_1)$.

The average Al/Si–O distances calculated from the final parameters are shown in Fig. 1(*a*). The Al/Si(1)–O distance lies between 1·63 and 1·75 Å while the Al/Si(2)–O, Al/Si(3)–O and Al/Si(4)–O distances vary from about 1·60 to 1·71 Å. This shows that the substitutional modulations of all the Al/Si sites are strong and the Al/Si ordering is almost complete.

The substitutional modulation waves for the Ca/Na sites were determined from the occupational parameters z_n^i ($i=1,2,3,4$ and $n=0,1$) introduced in *Refinement method*. The final occupational parameters for these sites are shown in Table 3. Of five parameters, only one, z_1^2, is reliable because the remaining parameters are less than their standard deviations. The parameter z_1^2 represents the amplitude of the substitutional modulation, which replaces Ca(1) with Na(1) and Ca(2) with Na(2) and *vice versa*. The total occupation probability of Ca in the split site, calculated by using only z_0^1, z_0^2 and z_1^2, is plotted in Fig. 1(*b*). This curve shows that the substitutional modulation of the Ca/Na sites is weak and almost in phase with the change in the interatomic distances of Al/Si–O.

Phase fluctuation

In the present analysis, the phase fluctuation of the modulation wave is not explicitly considered because the intensity data used include only those of the main and e_1-satellite reflections. In the following, the effect of the phase fluctuation is discussed, which is important for more accurate analysis with higher-order satellites and also for the interpretation of the present results.

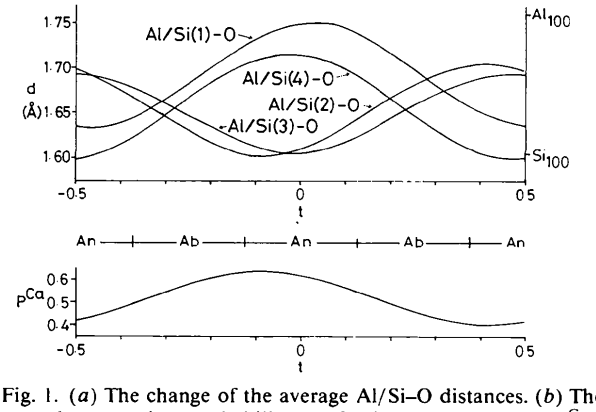

Fig. 1. (*a*) The change of the average Al/Si–O distances. (*b*) The total occupation probability of Ca in the split sites. $P^{Ca}=P^{Ca(1)}+P^{Ca(2)}$. P^{Na} is given by $1-P^{Ca}$. An and Ab represent the anorthite-like and albite-like regions.

As shown in the case of a Bravais lattice including only one atom in a unit cell by Overhauser (1971), the higher-order satellite intensity is drastically reduced by the phase fluctuation of the modulation wave. The structure factor of a reflection $h_1h_2h_3h_4$ is given by

$$F(h_1h_2h_3h_4)=F^0(h_1h_2h_3h_4)\exp(-B'_{44}h_4^2) \quad (11)$$

$$B'_{44}=2(\pi\Delta t)^2, \quad (12)$$

where $F^0(h_1h_2h_3h_4)$ is the structure factor when no phase fluctuation is taken into account and Δt is the standard deviation of the phase fluctuation, for which the Gaussian distribution is assumed. Formula (11) is correct for a general one-dimensionally modulated structure as is easily derived from a general structure factor formula (Yamamoto, 1982*a*). The last factor in (11) reduces preferentially the higher-order satellite intensity. In general, the magnitude of the phase fluctuation mode (phason) in the lattice vibrations is considered to be comparable with that of the usual phonon (Axe, 1980). In addition, the static phase fluctuation is commonly expected in the modulated structure where the cation ordering is an important factor of the modulation.

As observed in the structure images by electron microscopy, plagioclase consists of many coherent domains which have almost the same modulation period but have different phases. [See, for example, Fig. 2(*c*) in Wenk, Joswig, Tagai, Korekawa & Smith (1980).] Because the phase fluctuation reduces the effective amplitudes of the modulation waves, the amplitudes obtained from the structure analysis must be regarded as the effective amplitudes (Axe, 1980).

In the present case, the phase fluctuation is considered to be not strong from the Al/Si–O distances mentioned in *Modulated structure*. In order to check this, we refined B'_{44} together with other structural parameters by using (11). The refinement was initiated from the best parameters for $B'_{44}=0{\cdot}15$. After several cycles, B'_{44} almost vanished and the other parameters returned to almost the same values mentioned in *Structure refinement*. However, for all B'_{44} values, the R factor is not much different. This suggests that B'_{44} is strongly correlated with the other structural parameters. This occurs if $\mathbf{h}.\mathbf{u}^{\mu}\ll 1$ because then the structure factor almost linearly depends on the displacement $\mathbf{u}^{\mu}$ (Yamamoto, 1982*a*): infinite combinations of u_{in}^{μ} and B'_{44} giving the same $u_{in}^{\mu}\exp(-B'_{44}n^2)$ value lead to almost the same structure factor. In the present case, we used the reflections within $|h|<1{\cdot}3$ Å^{-1} and the average displacement is about 0·1 Å.

Therefore, the above condition is nearly fulfilled: $\mathbf{h}.\mathbf{u} < 0{\cdot}13$. For the determination of B'_{44}, the reflections with larger diffraction angles play an essential role.

In conclusion, it is generally necessary to consider, in the interpretation of the modulation waves, that the effective amplitudes are reduced by the phase fluctuation, particularly in the higher-order harmonics. In the present case, the phase fluctuation is considered to be not strong, though it definitely reduces the intensity of the higher-order satellite reflections.

Discussion

(*a*) *Modulated structure of labradorite*

We obtained strong substitutional modulation for all the Al/Si sites and weak substitutional modulation for the Ca/Na sites. The result is reasonably interpreted by the model proposed by Kitamura & Morimoto (1975, 1977). In this model (hereafter the KM model), the anorthite-like and albite-like bands alternate twice in a modulation period. To interpret the interatomic-distance curves (*d* curves) of Fig. 1 based on the KM model, the anorthite-like and albite-like bands are considered to be An_{80} and An_{20} respectively, from the possible phase relations of plagioclase (Smith, 1983; Grove, Ferry & Spear, 1983), and the lattice images of labradorite (Nakajima *et al.*, 1977). The *d* curves expected from this model are shown in Fig. 2. The idealized Al/Si distributions in An_{80} and An_{20} are shown in Fig. 3 from the mixing of the albite and anorthite structures. The substitutional modulations of Al/Si(3), Al/Si(4) sites implied by Fig. 2 are slightly stronger than the corresponding one in Fig. 1 and the average Al content in the Al/Si(1) site and the average Si contents in the Al/Si(2), Al/Si(3), and Al/Si(4) sites are larger than those in Fig. 1.

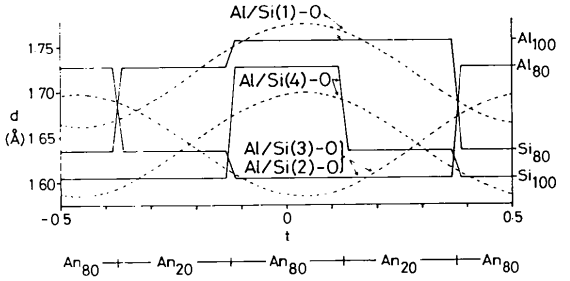

Fig. 2. The change of the average Al/Si–O distances predicted by the model of Kitamura & Morimoto (1977) (solid lines) and their harmonic parts (dotted lines). The anorthite-like and albite-like regions are represented by An_{80} and An_{20}.

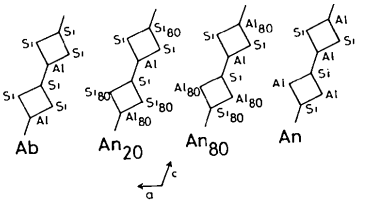

Fig. 3. The Al/Si distribution in the idealized An_{80} and An_{20} assumed to obtain the interatomic-distance curves of Fig. 2. The solid lines represent a schematic view of the chain of Al/Si–O tetrahedra along the *c* axis in feldspar (see Fig. 4). Al_{80} (Si_{80}) indicates that the site is occupied by Al (Si) and Si (Al) with occupation probabilities of 0·80 and 0·20.

The discrepancy in the change of Al/Si–O distances in Figs. 1 and 2 may partly be explained by the fact that the effective amplitudes of the modulation waves are reduced by the phase fluctuation. The discrepancy may also partly be due to the simplification in the modeling. In the calculation of the *d* curves in Fig. 2, we take Al/Si–O distances corresponding to the idealized Al/Si distribution for An_{80} and An_{20} (Fig. 3), where several sites are completely occupied by Si or Al. In the real anorthite-like and albite-like regions, these sites may partly be occupied by Al or Si (for example, Tagai, Joswig & Korekawa, 1980). The weak substitutional modulation of Ca/Na sites (Fig. 1*b*) does not contradict the KM model since the strong second-order harmonics, which are predicted for the substitutional modulation of these sites in this model, were not taken into account in this analysis.

Fig. 4 shows the structures in the middle of the anorthite-like ($t = 0$ in Fig. 2) and albite-like ($t = 0{\cdot}25$) regions calculated from the final parameters (Table 2) and symmetry operators mentioned previously. The

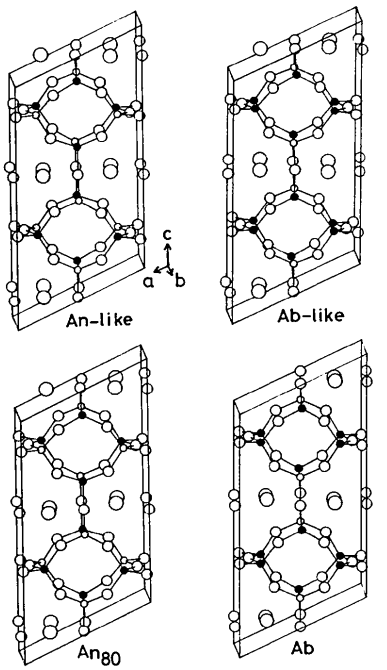

Fig. 4. Comparison of the structures in the anorthite-like region (t=0, An-like) and albite-like region (t=0·25, Ab-like) of labradorite (An_{52}) with the structures of a body-centered anorthite (An_{80}, Fleet *et al.*, 1966) and albite (Ab, Ribbe *et al.*, 1969). The large, medium and small circles represent Ca/Na, O and Al/Si sites, respectively. The Si-dominated Al/Si sites are shaded.

structures have strong resemblance to the body-centered anorthite (An_{80}) and albite (Fleet, Chandrasekhar & Megaw, 1966; Ribbe, Megaw & Taylor, 1969). The albite-like structure is, however, slightly different from the albite structure, particularly in the position of Ca/Na and the occupation probability of Ca (Fig. 1*b*). This is because the second-order harmonics have not been used in the present analysis as mentioned above. If these are included, the discrepancy may be removed. Thus the present result is well explained by the KM model.

(*b*) *Second-order harmonics of the modulation waves*

The interpretation described above is, however, not unique. If we assume a simple antiphase-domain model of the ideal An_{50} which can be obtained from the mixing of Ab and An structures, the model gives d curves for the Al/Si–O distances which are similar to those in this study within the harmonic approximation. This is the model presented by Horst *et al.* (1981) (hereafter the HTKJ model). The essential difference between these two models is in the presence of the second-order harmonics of the modulation waves: the KM model should have strong second-order harmonics while the HTKJ model should not. We could not, however, determine the amplitudes of the second-order harmonics because the e_2-satellite reflections were not included in the data used.

An attempt to determine the second-order harmonics was made by Toman & Frueh (1976). They refined the second-order harmonics using 318 e_2 satellites. Their d curves are analogous to those of the present result, indicating that the contribution of the second-order harmonics in the d curves is not great. However, the R factor of 0·27 for e_2 satellites indicates that the second-order harmonics obtained are not accurate. Therefore, we confine ourselves to the qualitative consideration of the higher-order satellite intensity.

We calculate the Fourier amplitudes of the average Al/Si–O distances up to the third-order harmonics in order to show how the KM model reasonably explains the diffraction aspect of the higher-order satellite reflections (Table 4). As shown in Table 4, the magnitudes of the second- and third-order harmonics are about one-half and one-third of that of the first-order harmonic. Therefore, the intensities of the e_2 and e_3 satellite reflections are expected to be of the order of $\frac{1}{4}$ and $\frac{1}{9}$, respectively, of the e_1 satellites. These ratios may be reduced further by the phase fluctuation mentioned above. The second-order harmonics of the substitutional modulation for the Ca/Na sites, expected from the model, may also contribute to the e_2 satellite intensity. The contribution of the substitutional modulation of only one Ca/Na atom cannot, however, be so large compared to that of the displacive modulations of all, 13, atoms. Thus, the relative intensities of the e_2 and e_3 satellites estimated above based on the KM model explain well the qualitatively known diffraction aspect. In fact, the e_3 satellites have not been observed by X-ray diffraction.

Table 4. *Fourier amplitudes of the average* Al/Si–O *distances obtained from the solid lines in Fig.* 2

The Al/Si–O distances are given by $d = a_0 + a_1 \cos(2\pi t) + b_1 \sin(2\pi t) + a_2 \cos(4\pi t) + a_3 \cos(6\pi t) + b_3 \sin(6\pi t)$. [The term $b_2 \sin(4\pi t)$ vanishes in the present case.]

	a_0	a_1	b_1	a_2	a_3	b_3
Al/Si(1)	1·719	0·0549	0·0135	−0·0293	0·0183	0·0045
Al/Si(2)	1·643	−0·0549	−0·0135	0·0293	−0·0183	−0·0045
Al/Si(3)	1·643	−0·0549	−0·0135	0·0293	−0·0183	−0·0045
Al/Si(4)	1·643	0·0549	0·0135	0·0293	0·0183	0·0045

The existence of the second-order harmonics in the modulation waves was shown by Toman & Frueh (1976). This is also confirmed by the present work. The diffraction harmonics calculated from the present harmonic model give too weak intensity for most e_2 satellite reflections. Therefore, the precise structure must be determined based on a model including the second-order harmonics as in the KM model and the analysis of the e_2 satellites considering the phase fluctuation is inevitable.

(*c*) *Antiphase-domain structure*

To explain the appearance of the second-order satellitè reflections, Horst *et al.* (1981) discussed the possibility of an antiphase-domain structure with an asymmetric box-type modulation. This structure can be expressed as a modulated structure with asymmetric box-type modulation waves for the displacive modulations when the substitutional modulation of the Ca/Na sites is neglected. Then, the structure consists of four different units, two pairs of which are related to the antiphase relation as in the case of the KM model because of the presence of the centering translations mentioned above. Therefore, the KM model is considered to be an example of the antiphase-domain structure with the asymmetric box-type modulation waves except for the substitutional modulation of the Ca/Na sites. However, the substitutional modulation for the Ca/Na sites is different between the HTKJ and KM antiphase-domain structure models. In the KM model, the second-order harmonic is dominant, while in the HTKJ model, the first-order harmonic is dominant because the modulation wave of the substitutional modulation is constrained by the modulation wave of the displacive modulation.

As discussed above, the contribution of the displacive modulation to the satellite intensity is considered to be predominant in comparison with that of the substitutional modulation. This is applicable not only to the e_1 satellite but also to the e_2 satellite. Therefore, the antiphase-domain structure with an asymmetric box-type modulation must be similar to the KM model in essential points.

(d) Crystal-chemical aspect

The structure of labradorite given by the present analysis or the KM model is quite different from those given by Toman & Frueh (1976) and Horst *et al.* (1981) from the crystal-chemical viewpoint.

Toman & Frueh obtained a strong displacive modulation giving an Al/Si distribution similar to the present one where the Al-rich regions alternate with the Si-rich regions twice in the modulation period. However, the first-order harmonic of the substitutional modulation for the Ca/Na site is also strong in contrast to the present result. In this case, if an independent Ca/Na site is Ca-rich, the site obtained from this site by the translation $(\mathbf{a}+\mathbf{b}+\mathbf{c})/2$ is also Ca-rich because the modulation wave of this site is obtained from that of the independent site by the centering translation $(\mathsf{E}|\frac{1}{2},\frac{1}{2},\frac{1}{2},0)$ and is the same as in the independent site. In contrast, the sites obtained from the independent site by the translations $(\mathbf{a}+\mathbf{b})/2$ and $\mathbf{c}/2$ are Na-rich because the modulation waves for these sites are obtained by $(\mathsf{E}|\frac{1}{2},\frac{1}{2},0,\frac{1}{2})$, $(\mathsf{E}|0,0,\frac{1}{2},\frac{1}{2})$ and have the phase difference π. Therefore, Ca and Na are distributed homogeneously in both regions and there are no anorthite-like and albite-like regions as a whole.

Horst *et al.* gave the antiphase-domain structure with a notably disordered Al/Si distribution and an almost completely disordered Ca/Na distribution. Each antiphase domain is anorthite-like in symmetry. Therefore, there is no albite-like region in this model and the structure is chemically homogeneous. The antiphase-domain model with an asymmetric box-type modulation wave mentioned above also gives a homogeneous Ca/Na distribution. This model can describe the Al/Si distribution similarly to that of the KM model, while the Ca/Na distribution is different because the substitutional modulation wave of the Ca/Na site is also of asymmetric box-type. Since the first-order harmonic is predominant in this modulation wave, Ca and Na are distributed almost homogeneously as in the Toman & Frueh model mentioned above. The slight change of the Ca/Na distribution between the Al-rich and Si-rich regions comes from the weak second-order harmonics.

In contrast to these models, the second-order harmonic of the substitutional modulation of the Ca/Na site is dominant in the KM model. Therefore, when the independent Ca/Na site is Ca(Na)-rich, the site obtained from this site by the translations $(\mathbf{a}+\mathbf{b})/2$ and $\mathbf{c}/2$ are also Ca(Na)-rich because $(\mathsf{E}|\frac{1}{2},\frac{1}{2},0,\frac{1}{2})$ and $(\mathsf{E}|0,0,\frac{1}{2},\frac{1}{2})$ give the same second-order harmonics for these sites as that of the independent site. (The phase difference is 2π for the second-order harmonics.) As a result, there appear distinct Ca-rich and Na-rich regions. The present analysis gave the structure which is reasonably interpreted by the KM model, where Ca is rich in the Al-rich regions forming the anorthite-like structure and Na is rich in the Si-rich regions forming the albite-like structure. Since the present work confirmed that the Al/Si ordering is almost complete, such a Ca/Na distribution is natural from the crystal-chemical point of view.

Summary and concluding remarks

The refinement of the modulated structure of An_{52} has been performed by using the newly developed restricted least-squares technique based on the four-dimensional description of the modulated structure and the centrosymmetric triclinic space group in a nonstandard setting, which has the centering translations but is group-theoretically equivalent to $P^{P\bar{1}}_{\bar{1}}$. The refinement converged smoothly to the final result, giving an R factor of 0·094 for 3102 e_1-satellite reflections. The result shows the strong substitutional modulation for all the Al/Si sites and the weak substitutional modulation for the Ca/Na sites. The structure determined in this investigation is consistent with the model proposed by Kitamura & Morimoto (1977) within the harmonic approximation. Taking into consideration the anharmonic terms in the modulation waves, the most probable structure is a modulated structure with albite-like (An_{20}) and anorthite-like (An_{80}) regions. The body-centered anorthite-like regions in an antiphase relation are coherently separated by albite-like regions. The diffraction aspect of the higher-order satellite reflections has been reasonably explained by this structure and the concept of the phase fluctuation of the modulation waves.

APPENDIX 1

To show that the space group employed in the text is equivalent to the space group $P^{P\bar{1}}_{\bar{1}}$ in the standard setting (de Wolff, Janssen & Janner 1981), we consider the relation between the unit vectors employed in the present paper and those of the standard setting. In the standard setting, the primitive cell is employed for the triclinic space group. We can adopt Megaw's (1960) cell for the standard setting. The unit vectors of Megaw's cell $\mathbf{A}, \mathbf{B}, \mathbf{C}$ are related to $\mathbf{a}, \mathbf{b}, \mathbf{c}$ in the present paper by

$$\begin{pmatrix}\mathbf{A}\\ \mathbf{B}\\ \mathbf{C}\end{pmatrix}=\begin{pmatrix}1 & 0 & 0\\ \frac{1}{2} & \frac{1}{2} & 0\\ \frac{3}{2} & \frac{1}{2} & \frac{1}{2}\end{pmatrix}\begin{pmatrix}\mathbf{a}\\ \mathbf{b}\\ \mathbf{c}\end{pmatrix}, \qquad (A1)$$

while their reciprocal unit vectors are related by

$$\begin{pmatrix}\mathbf{A}^*\\ \mathbf{B}^*\\ \mathbf{C}^*\end{pmatrix}=\begin{pmatrix}1 & -1 & 2\\ 0 & 2 & -2\\ 0 & 0 & 2\end{pmatrix}\begin{pmatrix}\mathbf{a}^*\\ \mathbf{b}^*\\ \mathbf{c}^*\end{pmatrix}. \qquad (A2)$$

In this setting, all the observed reflections are

expressed as

$$\mathbf{h} = H_1\mathbf{A}^* + H_2\mathbf{B}^* + H_3\mathbf{C}^* + H_4\mathbf{K} \qquad (A3)$$

with integers H_1, H_2, H_3, H_4 and $\mathbf{K} = \mathbf{b}^* - \mathbf{c}^* + \mathbf{k}$ and there are no extinction rules (Kitamura & Morimoto, 1977), indicating that the space group is $P^{P\bar{1}}_{\bar{1}}$ or P^{P1}_{1} depending on whether inversion symmetry is present or not. The four-dimensional unit vectors in this setting are defined by $\mathbf{A}_1 = \mathbf{A} - K_1\mathbf{d}$, $\mathbf{A}_2 = \mathbf{B} - K_2\mathbf{d}$, $\mathbf{A}_3 = \mathbf{C} - K_3\mathbf{d}$ and $\mathbf{A}_4 = \mathbf{d}$ where K_1, K_2, K_3 are the $\mathbf{A}^*$, $\mathbf{B}^*$, $\mathbf{C}^*$ components of $\mathbf{K}$, which are given from the definition of $\mathbf{K}$ by k_1, $(k_1+k_2+1)/2$, $(3k_1+k_2+k_3)/2$. Using (A1) and the above relations, the unit vectors $\mathbf{A}_1$, $\mathbf{A}_2$, $\mathbf{A}_3$, $\mathbf{A}_4$ are written in terms of the unit vectors $\mathbf{a}_1$, $\mathbf{a}_2$, $\mathbf{a}_3$, $\mathbf{a}_4$ used in the text as

$$\begin{pmatrix}\mathbf{A}_1\\ \mathbf{A}_2\\ \mathbf{A}_3\\ \mathbf{A}_4\end{pmatrix} = \begin{pmatrix}1 & 0 & 0 & 0\\ \frac{1}{2} & \frac{1}{2} & 0 & -\frac{1}{2}\\ \frac{3}{2} & \frac{1}{2} & \frac{1}{2} & 0\\ 0 & 0 & 0 & 1\end{pmatrix}\begin{pmatrix}\mathbf{a}_1\\ \mathbf{a}_2\\ \mathbf{a}_3\\ \mathbf{a}_4\end{pmatrix}. \qquad (A4)$$

We write this as $\mathbf{A}_i = \sum_j Q_{ij}\mathbf{a}_j$ in the following.

The relation (A4) clearly shows that $\mathbf{A}_i (i = 1, \ldots, 4)$ span the same lattice as in the text and both settings are equivalent to each other. This leads to the following transformation properties.

From (A2) and $\mathbf{K}$, their reciprocal vectors are related to $\mathbf{b}_1$, $\mathbf{b}_2$, $\mathbf{b}_3$, $\mathbf{b}_4$ by

$$\begin{pmatrix}\mathbf{B}_1\\ \mathbf{B}_2\\ \mathbf{B}_3\\ \mathbf{B}_4\end{pmatrix} = \begin{pmatrix}1 & 1 & -2 & 0\\ 0 & 2 & -2 & 0\\ 0 & 0 & 2 & 0\\ 0 & 1 & -1 & 1\end{pmatrix}\begin{pmatrix}\mathbf{b}_1\\ \mathbf{b}_2\\ \mathbf{b}_3\\ \mathbf{b}_4\end{pmatrix}. \qquad (A5)$$

This is expressed as $\mathbf{B}_i = \sum_j (\tilde{\mathrm{Q}}^{-1})_{ij}\mathbf{b}_j$ where $\tilde{\mathrm{Q}}$ is the transpose matrix of Q. The indices h_i are transformed by $H_i = \sum_j \mathrm{Q}_{ij}h_j$. This shows that only observed $h_1h_2h_3h_4$ reflections, which fulfill $h_1+h_2+h_3 = 2n$, $h_1+h_2+h_4 = 2n$ and $h_3+h_4 = 2n$, can be indexed by four integers H_1, H_2, H_3, H_4, indicating that Megaw's cell and wavevector $\mathbf{K}$ really give the standard setting with primitive cell and give rise to no extinction rule.

Now we consider the transformation properties of the coordinates. The coordinates X_i with respect to $\mathbf{A}_i (i = 1, \ldots, 4)$ are related to the coordinates x_i with respect to $\mathbf{a}_i (i = 1, \ldots, 4)$ by the matrix $\tilde{\mathrm{Q}}^{-1}$. In particular, we have $\bar{X}_4 = \bar{x}_2 - \bar{x}_3 + \bar{x}_4$ or $\bar{x}_4 = -\frac{1}{2}\bar{X}_2 + \bar{X}_4$. This gives the relation between the modulation functions in the standard setting and those in the setting employed in the text. For example, for the displacement at $\bar{X}_1\mathbf{A}_1 + \bar{X}_2\mathbf{A}_2 + \bar{X}_3\mathbf{A}_3 + \bar{X}_4\mathbf{A}_4 = \bar{x}_1\mathbf{a}_1 + \bar{x}_2\mathbf{a}_2 + \bar{x}_3\mathbf{a}_3 + \bar{x}_4\mathbf{a}_4$, we have

$$U_i(\bar{X}_4) = \sum_u (\tilde{\mathrm{Q}}^{-1})_{ij}u_i(-\tfrac{1}{2}\bar{X}_2 + \bar{X}_4) \qquad (A6)$$

and

$$u_i(\bar{x}_4) = \sum_j \tilde{\mathrm{Q}}_{ij}U_j(\bar{x}_2 - \bar{x}_3 + \bar{x}_4), \qquad (A7)$$

where U_i are the $\mathbf{A}_i$ components of the displacement.

From (A6) and (A7) we have the relations in the Fourier amplitudes: $U_{in} = \sum_j (\tilde{\mathrm{Q}}^{-1})_{ij}u_{jn}\exp(-\pi i n\bar{X}_2)$ and $u_{in} = \sum_j \tilde{\mathrm{Q}}_{ij}U_{jn}\exp[2\pi i n(\bar{x}_2 - \bar{x}_3)]$. Equation (A7) leads to the following relations. If the modulation function of an independent atom is $u_i(\bar{x}_4)$, the modulation function of the atom obtained from this atom by the translation $(\mathbf{a}+\mathbf{b}+\mathbf{c})/2$ is also $u_i(\bar{x}_4)$ while those of atoms obtained by the translations $(\mathbf{a}+\mathbf{b})/2$, $\mathbf{c}/2$ are $u_i(\bar{x}_4 + \frac{1}{2})$ and $u_i(\bar{x}_4 - \frac{1}{2})$. These are consistent with the relations obtained from the transformation property under the centering translations (see text).

Thus if we have the modulation waves in either of these settings, we can obtain those in the remaining setting by using (A6) or (A7) and the corresponding formulas for the temperature factor and the occupation probability. As shown above, the different setting leads to a different representation of the same structure.

APPENDIX 2

We consider the structure factor in order to show that the centering translations can be dropped in the structure factor calculation. The structure factor with isotropic temperature factors is given by the following formula (Yamamoto, 1982*a*)

$$\begin{aligned} F_{\mathbf{h}} = \sum_\mu \sum_{(\mathrm{R}|\boldsymbol{\tau})} a^\mu \int_0^1 \mathrm{d}\bar{x}_4^\mu f^\mu(\mathbf{h}) P^\mu(\bar{x}_4^\mu) \\ \times \exp\{-B^\mu(\bar{x}_4^\mu)h^2/4 + 2\pi i \\ \times \sum_{j=1}^{4} h_j[\mathrm{R}\bar{\mathbf{x}}^\mu + \mathrm{R}\mathbf{u}^\mu(\bar{x}_4^\mu) + \boldsymbol{\tau}]_j\}, \end{aligned} \qquad (A8)$$

where a^μ is the multiplicity of the μth independent atom, $f^\mu(\mathbf{h})$ is the atomic scattering factor, $\bar{\mathbf{x}}^\mu = \bar{x}_1^\mu\mathbf{a}_1 + \bar{x}_2^\mu\mathbf{a}_2 + \bar{x}_3^\mu\mathbf{a}_3 + \bar{x}_4^\mu\mathbf{a}_4$ and $\bar{x}_1^\mu$, $\bar{x}_2^\mu$, $\bar{x}_3^\mu$ are the atomic coordinates in the average structure. The summation with respect to μ runs over all the independent atoms while the sum of $(\mathrm{R}|\boldsymbol{\tau})$ is taken over all the symmetry operators which generate new atoms in the unit cell from the independent atoms. We can, however, drop the centering translations if the extinct reflections due to these translations are not included in the reflection data used because of the following reason.

We consider the set G of all the symmetry operators which generate new atoms in a unit cell from the independent atoms. Then G can be divided into four cosets by use of the centering translations:

$$\begin{aligned} \mathrm{G} = (\mathrm{E}|0,0,0,0)\mathrm{G}_0 + (\mathrm{E}|\tfrac{1}{2},\tfrac{1}{2},\tfrac{1}{2},0)\mathrm{G}_0 \\ + (\mathrm{E}|\tfrac{1}{2},\tfrac{1}{2},0,\tfrac{1}{2})\mathrm{G}_0 + (\mathrm{E}|0,0,\tfrac{1}{2},\tfrac{1}{2})\mathrm{G}_0, \end{aligned} \qquad (A9)$$

where G_0 is a set of $(\mathrm{E}|0,0,0,0)$ and $(\mathrm{I}|0,0,0,0)$ in the present case.

We write a part of the structure factor obtained from (A8) by summing over the elements of G_0 as

$F'_{\mathbf{h}}$. Then the structure factor is given by

$$F_{\mathbf{h}} = F'_{\mathbf{h}}[1 + \exp \pi i(h_1 + h_2 + h_3) + \exp \pi i(h_1 + h_2 + h_4) + \exp \pi i(h_3 + h_4)]. \quad (A10)$$

Here the second, third and fourth terms correspond to the contribution from the summation over the elements of three cosets $(\mathrm{E}|\frac{1}{2}, \frac{1}{2}, 0)\mathrm{G}_0$, $(\mathrm{E}|\frac{1}{2}, \frac{1}{2}, 0, \frac{1}{2})\mathrm{G}_0$ and $(\mathrm{E}|0, 0, \frac{1}{2}, \frac{1}{2})\mathrm{G}_0$. The last factor in (A10) gives the extinction rules $h_1 + h_2 + h_3 = 2n$, $h_1 + h_2 + h_4 = 2n$, $h_3 + h_4 = 2n$ and for the reflections which fulfill these conditions, this takes 4. Therefore the structure factor is calculated only by taking into account the symmetry operator in G_0. This is analogous to the situation in the usual three-dimensional centered lattice.

References

AXE, J. D. (1980). *Phys. Rev. B*, **21**, 4181–4190.

BOWN, M. G. & GAY, P. (1958). *Z. Kristallogr.* **111**, 1–14.

FLEET, S. G., CHANDRASEKHAR, S. & MEGAW, H. D. (1966). *Acta Cryst.* **21**, 782–801.

GROVE, T. L., FERRY, J. M. & SPEAR, F. S. (1983). *Am. Mineral.* **68**, 41–59.

HAMILTON, W. C. (1965). *Acta Cryst.* **18**, 502–510.

HORST, W., TAGAI, T., KOREKAWA, M. & JAGODZINSKI, H. (1981). *Z. Kristallogr.* **157**, 233–250.

JANNER, A. & JANSSEN, T. (1977). *Phys. Rev. B*, **15**, 643–658.

KITAMURA, M. & MORIMOTO, N. (1975). *Proc. Jpn Acad.* **51**, 419–424.

KITAMURA, M. & MORIMOTO, N. (1977). *Phys. Chem. Miner.* **1**, 199–212.

KOREKAWA, M. & JAGODZINSKI, H. (1967). *Schweiz. Mineral. Petrogr. Mitt.* **47**, 269–278.

MEGAW, H. D. (1960). *Proc. R. Soc. (London) Ser. A*, **259**, 159–183.

MORIMOTO, N. (1979). *AIP Conf. Proc.* No. 53, pp. 299–310.

MORIMOTO, N., NAKAJIMA, Y. & KITAMURA, M. (1975). *Proc. Jpn Acad.* **51**, 725–728.

NAKAJIMA, Y., MORIMOTO, N. & KITAMURA, M. (1977). *Phys. Chem. Mineral.* **1**, 213–225.

OVERHAUSER, A. W. (1971). *Phys. Rev. B*, **3**, 3173–3182.

RIBBE, P. H. & GIBBS, G. V. (1969). *Am. Mineral.* **54**, 85–94.

RIBBE, P. H., MEGAW, H. D. & TAYLOR, W. H. (1969). *Acta Cryst.* B**25**, 1503–1518.

SMITH, J. V. (1983). Abstr. 3rd NATO Advanced Study, Institute of Feldspars. *Feldspars and Their Paragenesis*, 32.

TAGAI, T. (1980). *Die Untersuchung der modulierten Kristallstrukturen des intermediaren Plagioklases* An_{52}. Thesis, Frankfurt Univ.

TAGAI, T., JOSWIG, W. & KOREKAWA, M. (1980). *Z. Kristallogr.* **151**, 77–89.

TOMAN, K. & FRUEH, A. J. (1973). *Z. Kristallogr.* **138**, 337–342.

TOMAN, K. & FRUEH, A. J. (1976). *Acta Cryst.* B**32**, 526–538.

WENK, H., JOSWIG, W., TAGAI, T., KOREKAWA, M. & SMITH, K. B. (1980). *Am. Mineral.* **65**, 81–95.

WOLFF, P. M. DE (1974). *Acta Cryst.* A**30**, 777–785.

WOLFF, P. M. DE, JANSSEN, T. & JANNER, A. (1981). *Acta Cryst.* A**37**, 625–636.

YAMAMOTO, A. (1982*a*). *Acta Cryst.* A**38**, 87–92.

YAMAMOTO, A. (1982*b*). *Acta Cryst.* B**38**, 1446–1451.

YAMAMOTO, A. & INOUE, Z. (1981). *Acta Cryst.* A**37**, 838–842.

YAMAMOTO, A. & NAKAZAWA, H. (1982). *Acta Cryst.* A**38**, 79–86.

Acta Cryst. (1984). B**40**, 237–244

A High-Resolution Electron Microscopy Study of Disorder in Two Types of Rutile-Related Crystallographic-Shear Phases

BY L. C. OTERO-DIAZ* AND B. G. HYDE

Research School of Chemistry, Australian National University, GPO Box 4, Canberra, ACT Australia

(*Received* 10 *October* 1983; *accepted* 3 *January* 1984)

Abstract

Two specimens were studied: rutile that had been melted in an argon-arc furnace, and therefore slightly reduced, and a V_2O_3-doped TiO_2 of nominal composition $(V, Ti)O_{\sim 1.875}$ which had been quenched from 1873 K. Both were examined at the atomic-resolution level. The former contained only a few areas with crystallographic-shear planes, and these were roughly parallel to $(1\bar{3}2)_r$, and appeared quite 'thick' in projection along $[1\bar{1}1]_r$. (The subscript r indicates the rutile subcell.) The latter contained a $(253)_r$ crystallographic-shear structure with $n \approx 23$. In both cases the crystallographic-shear planes showed variations in orientation. A tentative explanation of the observed phenomena is proposed. [Crystal data for the first specimen: $a = 4{\cdot}5940\,(1)$, $c = 2{\cdot}9600\,(1)$ Å, $V = 62{\cdot}4688\,(2)$ Å^3.]

1. Introduction

The titanium oxide ('reduced rutile') system has been extensively studied for half a century, and is established as a prototype case in which there are sequences of ordered structures with definite but 'grotesque' stoichiometries. From $TiO_{1.750}$ to $TiO_{1.889}$ the

* Present addresses: Departamento de Química Inorgánica, Facultad de Ciencias Químicas, Universidad Complutense, Madrid-3, and Instituto de Química Inorgánica Elhuyar CSIC, Serrano 113, Madrid-6, Spain.

0108-7681/84/030237-08$01.50